

UNCLASSIFIED

BIC FILE COR

AD-A200 119

REPORT DOCUMENTATION PAGE

(2)

2a SECURITY CLASSIFICATION AUTHORITY TIC		1d RESTRICTIVE MARKINGS	
2b DECLASSIFICATION/DOWNGRADING SCHEDULE SELECTED SEP 13 1988		3 DISTRIBUTION/AVAILABILITY OF REPORT APPROVED FOR PUBLIC RELEASE DISTRIBUTION IS UNLIMITED	
4 PERFORMING ORGANIZATION REPORT NUMBER D-4		5 MONITORING ORGANIZATION REPORT NUMBER AFOSR-TR- 88-1153	
6a NAME OF PERFORMING ORGANIZATION Prof. Richard B. Miles Princeton University, MAE Dept.	6b OFFICE SYMBOL (if applicable)	7a NAME OF MONITORING ORGANIZATION AFOSR/NA	
6c ADDRESS (City, State and ZIP Code) Princeton University, MAE Dept. D-414 Engineering Quad., Olden St. Princeton, NJ 08544		7b ADDRESS (City, State and ZIP Code) BUILDING 410 BOLLING AFB, DC 20332-6448	
8a NAME OF FUNDING/SPONSORING ORGANIZATION AFOSR/NA	8b OFFICE SYMBOL (if applicable) NA	9 PROCUREMENT INSTRUMENT IDENTIFICATION NUMBER AFOSR-86-0191	
8c ADDRESS (City, State and ZIP Code) BUILDING 410 BOLLING AFB, DC 20332-6448		10 SOURCE OF FUNDING NOS	
		PROGRAM ELEMENT NO. 61102F	PROJECT NO. 2307
		TASK NO. A2	WORK UNIT NO.
11. TITLE (Include Security Classification) Development & Application (U) Oxygen Flow Tagging for Velocity Measurements & Flow Visualization in Turbulent 3-D Supersonic Flows			
12. PERSONAL AUTHOR(S) Miles, Richard B.			
13a TYPE OF REPORT Annual Tech. Report	13b TIME COVERED FROM 6/1/87 TO 5/31/88	14 DATE OF REPORT (Yr., Mo., Day) 9/14/88	15 PAGE COUNT 38
16 SUPPLEMENTARY NOTATION			
17 COSATI CODES		18 SUBJECT TERMS (Continue on reverse if necessary and identify by block number)	
FIELD	GROUP	SUB GR	
		Flow Diagnostics; Velocity Measurements; Temperature Measurements; Density Measurements; Laser Diagnostics; Supersonic Flows.	
19. ABSTRACT (Continue on reverse if necessary and identify by block number) During the past year our major accomplishment has been the demonstration of the oxygen flow tagging under conditions which duplicate the Mach 3 facility, at the Princeton Gas Dynamics Laboratory. These tests were done in an underexpanded axisymmetric jet up to Mach 4. We have been able to take velocity data through the core and across the free shear layer of this jet and have generated images of instantaneous flow structure from which we have computed the average velocity profiles, turbulence intensity, and the axial velocity correlations. We have succeeded in doing simultaneous two-line flow tagging and have used that data to generate stream-wise velocity correlations in the same axisymmetric jet. The data which has been generated has been compared with a high-speed subsonic jet to give us a quantitative measure of the difference between supersonic and subsonic turbulence.			
20 DISTRIBUTION/AVAILABILITY OF ABSTRACT UNCLASSIFIED/UNLIMITED <input checked="" type="checkbox"/> SAME AS RPT <input type="checkbox"/> DTIC USERS <input type="checkbox"/>		21 ABSTRACT SECURITY CLASSIFICATION UNCLASSIFIED	
22a NAME OF RESPONSIBLE INDIVIDUAL LON SAKELL JAMES M. MCMICHAEL		22b TELEPHONE NUMBER (include Area Code) 202-767-4935	22c OFFICE SYMBOL AFOSR/NA

DU FORM 1473, 83 APR

EDITION OF 1 JAN 73 IS OBSOLETE

UNCLASSIFIED

SECURITY CLASSIFICATION OF THIS PAGE

88 1011 T92

DEVELOPMENT AND APPLICATION OF OXYGEN FLOW TAGGING
FOR VELOCITY MEASUREMENTS AND FLOW VISUALIZATION IN
TURBULENT THREE-DIMENSIONAL SUPERSONIC FLOWS

Richard B. Miles
Mechanical & Aerospace Engineering
PRINCETON UNIVERSITY
Princeton, NJ 08544

September 14, 1988



Accession For	
NTIS GRA&I	<input checked="" type="checkbox"/>
DTIC TAB	<input type="checkbox"/>
Unannounced	<input type="checkbox"/>
Justification	
By	
Distribution/	
Availability	
Avail and/or	
Special	
A-1	

ABSTRACT

During the past year our major accomplishment has been the demonstration of the oxygen flow tagging under conditions which duplicate the Mach 3 facility at the Princeton Gas Dynamics Laboratory. These tests were done in an underexpanded axisymmetric jet up to Mach 4. We have been able to take velocity data through the core and across the free shear layer of this jet and have generated images of instantaneous flow structure from which we have computed the average velocity profiles, turbulence intensity, and the axial velocity correlations. We have succeeded in doing simultaneous two-line flow tagging and have used that data to generate stream-wise velocity correlations in the same axisymmetric jet. The data which has been generated has been compared with a high-speed subsonic jet to give us a quantitative measure of the difference between supersonic and subsonic turbulence.

A. FACILITIES DEVELOPMENT

Following the installation of the UV-quartz windows, the wind tunnel has been operated on a daily basis using our 1/4" sonic orifice as well as our contoured Mach 2 nozzle. Virtually all of the work done during the past year has used the sonic orifice operating with a plenum pressure to exit pressure ratio of 10.2:1. This produces a jet which expands to approximately Mach 4.1 just before the Mach disk. We are particularly interested in observing the region in the vicinity of Mach 3 and greater since this constituted a trial configuration for the Mach 3 facility at the Gas Dynamics Laboratory. Following our initial measurements, we modified the laser system to allow us to do simultaneous two-line marking. This involved placing a highly reflecting mirror on the far side of the tunnel and reflecting the pumping beams back through to mark a second line in the

flow. We also reconfigured the incident lasers so that they crossed, marking a short line segment. These lasers were then individually reflected back through the jet causing three more crossing points, to produce a total of four short line segments which could be simultaneously written into the flow field. These line segments have the potential of giving point vorticity measurements since they act as small "paddle wheels" and move and rotate as the flow field evolves.

A major rebuilding of our argon-fluoride laser was also necessary due to poor injection locking and low oscillator power. This was done by Lambda Physik and involved reworking the electrodes of the oscillator. We are currently investigating the possibility of replacing the argon-fluoride laser with a high-intensity UV flashlamp source. If this is possible, it would be a major simplification.

B. COMPUTER SOFTWARE

During the past year we have developed a versatile computer software package which has been used to do our data reduction and image processing. Images are acquired at the 10 Hz repetition rate of the laser systems and are downloaded from the videocamera to a frame grabber and then stored on videotape. The videotape provides a permanent record of the data. Computer processing is then done off-line by reading the videotape. The computer program can extract a small rectangular window from each image and rapidly transfer that data into the memory of the SUN 3/160 computer. The window can be selected to include that portion of the line of interest, and, in the case where two lines are simultaneously marked, the window can be expanded to include both. The number of such images transferred into the memory is only limited by the size of the window and the size of the memory.

In general, we have been able to process on the order of 100 images at a time. The computer program has the following features:

1. Automatic Line Identification. After the data is loaded into the computer, the location of the lines is determined by searching for the brightest pixel in each subsequent vertical row of pixels while stepping through each image window from left to right. The search is weighted towards the point located in the previous vertical row of pixels to favor continuity of the line. This also allows multiple lines to be tracked on the same image and eliminates random jumps to bright noise spots far from the tagged line. The center of the line is determined using a weighted sum of the pixels surrounding the brightest pixel.

2. Line Checking and Correction. Following the line identification, the image windows are displayed by the computer with the identified line location shown superimposed on the original data. Each individual image can be reviewed to insure that the line or lines identified do, in fact, lie on top of the recorded lines in the image. If not, in our early data the image was deleted. More recently, the program has been updated to permit the line

marking to be hand-corrected on a point-by-point basis so that the image can be used if the researcher is able to identify the line. Otherwise, the image can be deleted.

3. Average Velocity Profiles and Turbulence Intensity. Once the lines have been identified and verified, the computer calculates the average velocity profile and the root mean square of the velocity which gives the turbulence intensity. This may either be displayed as the root mean square of the velocity or as the ratio of the root mean square to the average velocity, giving the turbulence intensity in dimensionless units.

4. Velocity Correlations. Any point across the line can then be selected using a curser and the computer calculates the correlation between the velocity at that point in the velocity profile and with velocity at every other point. This gives a quantitative measure of the turbulence scale. When two lines are marked, the computer will also calculate the correlation of the velocity across the other line with the velocity at the selected point, giving the stream-wise correlation.

5. Velocity Histogram. Any point across the velocity profile can be chosen with the curser and the computer will generate a velocity histogram at that point showing the frequency of occurrence of the various values of the stream-wise velocity component at that same point in each of the recorded images.

6. Variance Histogram. The computer will calculate the total variance of each image from the average profile. A histogram of these variances is then plotted so that images which might be related to "bursting" can be identified. If any portion of this histogram is selected by the curser, the recorded images, together with superimposed average velocity profiles, are shown on the screen so that individual structures can be examined. This can be done iteratively to generate collages of such images.

7. Collage Generation. All of the images may be reviewed either in their originally grabbed form or in the form with the computer-identified line superimposed. During this review any of the images can be selected and made into a collage so that particularly interesting structures can be viewed.

8. Hydrogen Bubble Applications. The entire image field can be rotated and configured to do hydrogen bubble identification and line tracking using all the previously mentioned features. This has been done for the data analysis which will be presented in a thesis by Laura Sabadell under the direction of Alexander Smits.

C. RESEARCH RESULTS

The major research results are summarized in the two Appendices which are preprints of articles submitted for publication. The first is entitled, "Instantaneous Supersonic Velocity Profiles in an Underexpanded Sonic Jet by Oxygen Flow Tagging." It shows the results of the single line measurements across the supersonic free shear layer in our underexpanded sonic jet. The

flow was observed both before and after the Mach disk and centerline velocities, as well as turbulent structure, and statistics were recorded. This paper has been accepted for publication in Physics of Fluids. The second paper is entitled, "Instantaneous Profiles and Turbulence Statistics of Supersonic Free Shear Layers by Raman Excitation + Laser-Induced Electronic Fluorescence (RELIEF) Velocity Tagging of Oxygen." This paper has been submitted to the 11th Symposium on Turbulence to be held in Rolla, Missouri in October of this year. It is also to be reviewed for publication in Experiments in Fluids. This paper presents our results using two-line tagging across supersonic and subsonic axisymmetric jets. In this case the turbulence intensities across the free shear layer show some difference between supersonic and subsonic turbulence as do the velocity correlation functions.

We have submitted abstracts of our work for presentation at the 41st Annual Meeting of the Division of Fluid Dynamics of the American Physical Society, scheduled in Buffalo, New York in late November. Those abstracts are also included in Appendix 3.

D. ON-GOING RESEARCH

We are currently doing measurements of the velocity profiles, step-by-step from the exit of the nozzle up to the Mach disk in the underexpanded jet to determine details of the evolution of the free shear layer. We will also repeat this work to follow the evolution of the free shear layer in our Mach 2 supersonic nozzle which can be pressure-matched at the exit.

We are, at the same time, developing the capability of measuring time-averaged temperatures by scanning the dye laser and recording the intensity of the line as a function of dye laser frequency. The variation of the intensity is associated with the rotational population of the vibrationally excited state and is, consequently, a measure of the temperature of the flow. Other projects which we hope to do include vorticity measurements by short line segment marking and conditional sampling.

The installation of the facilities at the Gas Dynamics Laboratory is expected to begin in late Fall and preliminary experiments are scheduled for the Spring of 1989.

E. PUBLICATIONS AND REPORTS

1. "Multi-Point Oxygen Flow Tagging by Raman Excitation + Laser-Induced Electronic Fluorescence," R. Miles, November 24-26, 1985, Thirty-Eighth Meeting of the Division of Fluid Dynamics, American Physical Society, Bulletin of the American Physical Society 30, Paper CH-3, Page 1720, New York: American Physical Society, 1985.
2. "Oxygen Flow Tagging by Raman Excitation Plus Laser-Induced Electronic Fluorescence," R. Miles, June 1986, CLEO'86/IQEC'86, Conference on Lasers and Electro-Optics, San Francisco, California (Invited Paper).

3. "Time Resolved Velocity Profiles by Vibrational Tagging of Oxygen," R. Miles, J. Connors, S. Huang, E. Markovitz, and G. Russell, April 1987, CLEO'87/IQEC'87, Conference on Lasers and Electro-Optics, Baltimore, Maryland (Post Deadline Paper).
4. "Velocity Measurements by Vibrational Tagging and Fluorescent Probing of Oxygen," R. Miles, G. Cohen, J. Connors, P. Howard, S. Huang, E. Markovitz, and G. Russell. Optics Letters 12, 1987, page 861.
5. "Instantaneous 2D Temperature and Density Measurements in Oxygen and Air," R. Miles, J. Connors, E. Markovitz, G. Roth, and P. Howard. 40th Anniversary Meeting of the Division of Fluid Dynamics of the American Physical Society, Eugene, Oregon, November 22-24, 1987.
6. "Coherent Anti-Stokes Raman Scattering (CARS) and Raman Pumping Line Shapes in High Fields," R. Miles, J. Connors, E. Markovitz, and P. Howard. SPIE's O-E/LASE'88 Third Annual Technical Symposium on Optoelectronics and Laser Applications in Science and Engineering, Los Angeles, California, January 10-15, 1988 (Invited Paper).
7. "Proposed Single-Pulse Two-Dimensional Temperature and Density Measurements of Oxygen and Air," R. Miles, J. Connors, P. Howard, E. Markovitz, and G. Roth. Optics Letters 13, 1988, page 195.
8. "Instantaneous Supersonic Velocity Profiles in an Underexpanded Jet by Oxygen Flow Tagging," R. Miles, J. Connors, E. Markovitz, P. Howard and G. Roth. (Accepted for publication in Physics of Fluids).
9. "Instantaneous Profiles and Turbulence Statistics of Supersonic Free Shear Layers by Raman Excitation + Laser-Induced Electronic Fluorescence (RELIEF) Velocity Tagging of Oxygen," R.B. Miles, J.J. Connors, E.C. Markovitz, P.J. Howard, and G.J. Roth. Eleventh Symposium on Turbulence, Rolla, Missouri, (Submitted for publication in Experiments in Fluids).
10. "Three-Dimensional Quantitative Flow Diagnostics," R. Miles and D. Nosenchuck. Lecture Notes in Engineering: Advances in Fluid Mechanics Measurements, Ed. M. Gad-El-Hak, Springer-Verlag, New York, (1988?). (Invited Paper--In Preparation.)
11. "Instantaneous Supersonic Velocity Profiles by Oxygen Tagging," R. Miles. 1988 AFOSR Contractors Meeting on Turbulence, University of Southern California, Los Angeles, CA June 18-30, 1988.
12. "Instantaneous and Time-Averaged Turbulent Structure in the Free Shear Layer of an Underexpanded Supersonic Air Jet," E. Markovitz, J. Connors, G. Roth, P. Howard, and R. Miles. (To be presented at the 41st Annual Meeting of the Division of Fluid Dynamics of the American Physical Society, Buffalo, New York, November 1988.)

13. "Instantaneous Velocity Profiles and Density Cross Sections in High-Speed Air By RELIEF," J. Connors, E. Markovitz, G. Roth, P. Howard, and R. Miles. (To be presented at the 41st Annual Meeting of the Division of Fluid Dynamics of the American Physical Society, Buffalo, New York, November 1988.)

PRESENTATIONS

1. "Instantaneous Two-Dimensional Temperature and Density Measurements in Oxygen and Air," R. Miles. American Physical Society Division of Fluid Dynamics Meeting, Eugene, Oregon, September 23, 1987.
2. "Acquisition and Visualization of Three-Dimensional Fluid Dynamics Data," R. Miles. Lehigh University, January 29, 1988.
3. "Instantaneous Supersonic Velocity and Density Profiles by RELIEF," R. Miles, Stanford University, March 25, 1988.
4. "Acquisition and Visualization of Fluid Dynamic Data: 1. Instantaneous Supersonic Velocity Profiles by RELIEF, 2. Projection of Space-Filling, Three-Dimensional Data," R. Miles. United Technologies, June 10, 1988.
5. "Instantaneous Supersonic Velocity Profiles by Oxygen Tagging," R. Miles, AFOSR Contractors Meeting, June 27-29, 1988, Los Angeles, California.
6. "Instantaneous Supersonic Velocity Profiles in Air by Oxygen Flow Tagging," R. Miles, NASA Langley, July 19, 1988.
7. "Velocity Profiles in Supersonic Air by O₂ RELIEF"; "Velocity Profiles in Proof-of-Concept Module (POCM) Exhaust by H₂ RELIEF"; and "Instantaneous H₂, O₂, and N₂ Density and Temperature Cross Sections by Single and Multiple Laser-Induced Fluorescence"; R. Miles. Exhaust Diagnostics Workshop, AEDC, Tennessee, August 23-24, 1988.

F. PERSONNEL

Graduate Students: Edward Markovitz and John Connors--completing Masters Degrees, Fall 1988. Gregory Russell--completing Ph.D., Fall 1988. Barry Zhang and Vinod Kumar--entering 1988.

Technician: Phil Howard--full time.

Research Scientist: Walter Lempert--joined our group as of July 1, 1988.

Undergraduate Contributors: Gregory Roth--computer program development.

INSTANTANEOUS SUPERSONIC VELOCITY PROFILES IN AN
UNDEREXPANDED SONIC JET BY OXYGEN FLOW TAGGING

Richard B. Miles
John Connors
Edward Markovitz
Philip Howard
Gregory Roth

PRINCETON UNIVERSITY
Department of Mechanical & Aerospace Engineering
Princeton, NJ 08544

(Submitted to Physics of Fluids)

ABSTRACT

The statistics and structure of velocity profiles across the free shear layer of a sonic free jet are examined using oxygen tagging by Raman excitation plus laser-induced electronic fluorescence. The flow is observed both before and after the Mach disk at centerline Mach numbers of 3.6 and .4, respectively. Instantaneous images of the displaced line of tagged molecules show a clear picture of the turbulent structure including large-scale coherent features.

PACS Numbers 47.25.Gk, 47.40.Ki, 42.65.Dr, 06.30.Gv

The recently developed Raman Excitation + Laser Induced Electronic Fluorescence (RELIEF) method of tagging oxygen molecules (1) provides a powerful tool for studying turbulent structure in high-speed flows. Time lines are written and tracked in air much as the hydrogen bubble technique (2) writes and tracks lines in water. Instantaneous images of velocity profiles as well as statistical characterizations can be made. No seeding is required.

The work reported here seeks to measure the turbulent structure in the free shear layer of an underexpanded sonic jet. Sonic jets have attracted attention from the early days, including work by E. Mach and Salcher (3) and Prandtl (4). Density profiles of these jets were determined interferometrically approximately 40 years ago (5). More recently, computational codes have been developed to elucidate both structure and the dynamic behavior (6,7). Experimental studies have relied principally on hot wire anemometers, schlieren, shadowgraph, interferometry, and laser velocimetry. In the last few years, laser-induced fluorescence has been used to generate time-averaged temperature and velocity field measurements in underexpanded jets including nitrogen seeded with sodium (8), and iodine (9,10), and air seeded with iodine (11).

The structural features of an underexpanded jet are shown in Fig. 1. The size and shape of the features are determined by the ratio of the jet exit pressure to the ambient pressure. In an underexpanded jet, the jet pressure at the nozzle exit is greater than the ambient pressure and, consequently, the jet undergoes a Prandtl-Meyer expansion. The associated

expansion fan reflects off the jet boundary, creating an incident shock wave (barrel shock) which, in turn, reflects off the Mach disk. There is a slip line behind the Mach disk which separates the still supersonic flow around the edge of the jet from the subsonic flow behind the normal shock. The jet boundary is a free shear layer, which is Kelvin-Helmholtz unstable.

Our measurements were taken in air with an operating pressure ratio of 10.2 (150 psia in the stagnation chamber exhausting into 1 atm), and a stagnation temperature of 250 K. The nozzle diameter was 6.35 mm (.25"). A computational model with these jet parameters was run using the SPF2 code (7). Table I shows the computed centerline velocity, temperature, pressure, density, and Mach number as a function of the distance from the nozzle. The Mach disk is predicted to be at 12.6 mm (.497") from the nozzle exit.

The experimental layout is shown in Fig. 2. Tagging is done by stimulated Raman excitation and requires a pair of synchronized, high-power pulsed lasers separated in frequency by the vibrational energy of the oxygen molecule (1555 cm^{-1}). We used a Quantel Model YG592 Nd:YAG/dye laser system injection locked with a Lightwave single frequency diode pumped Nd:YAG laser. This system was run with 50 mJ of doubled Nd:YAG laser light at $.532 \text{ }\mu\text{m}$ (green) and 40 mJ of dye laser light at $.580 \text{ }\mu\text{m}$ (orange) passing through the test cell. Figure 3 is an orthographic projection of the test region. The two tagging lasers were overlapped and focused to a waist approximately 50 microns in diameter, so they excite a thin line passing through the test region. Since the Nd:YAG laser also drives the

dye laser, the two laser pulses are automatically synchronized and, by using a delay line, can be made to reach the test section simultaneously. The tagging pulses are 10 nanoseconds in duration, so the flow moves only a few tens of microns during the tagging interval. The long vibrational lifetime of oxygen (12) assures that these molecules remain excited as they move downstream. The lasers pump the molecules into the same rotational state that they were in initially, so there is virtually no heating of the flow due to tagging.

After being tagged, the vibrationally excited molecules move with the flow for a time interval, Δt , and are then interrogated with a Lambda Physik EMG 150 MSC injection-locked argon-fluoride Excimer laser. This laser operates in the vicinity of $.193 \mu\text{m}$ (far ultraviolet) and is tuned to further excite only the $v = 1$ molecules up to the B state of oxygen (the Schumann-Runge band) from which they fluoresce. The fluorescence is detected with a gated and intensified UV-sensitive camera. As shown in Fig. 3, the interrogation laser is focused to a vertical sheet which intersects the jet longitudinally, so the motion of the line in the downstream direction can be seen. If no blocking far UV filter is used, direct Rayleigh scattering of the argon-fluoride Excimer laser light from the air molecules is also recorded on the camera, simultaneously giving a qualitative map of the density cross section of the jet in the interrogation plane. For the measurements, a $2 \mu\text{sec}$ time interval was used, and velocity variations were assumed to be only in u , the axial component of the velocity.

Images were grabbed into a Sun 3/160 computer, either real-time from the

camera or from a videotape. For each run, a baseline was recorded and a calibrated ruler was imaged for quantitative measurements. The timing between the tagging and interrogation laser pulses was controlled by a precision delay generator and was accurate to ± 5 nsec, the time jitter of the ArF laser. The $\Delta t = 0$ timing was checked with a fast optical diode and oscilloscope. The lasers operated at 10 Hz. After recording a series of images, the computer searched each image for the tagged line and then found the average velocity profile, the turbulence intensity profile, and the point-to-point correlations. Each image was reviewed after the computer located the tagged line to assure that no anomalous results were included in the statistics. Improperly digitized images were eliminated before the statistics were done.

Figures 4a through 4d were taken without a blocking filter so both the tagged line and the density cross section were recorded. The round feature in the lower portion of the figures is an artifact due to strong light scattering. The tagged line can be clearly seen in each of the figures. The sharp velocity drop across the slip lines behind the Mach disk is apparent in Figure 4c and 4d. The turbulence of the jet boundary is apparent in all the pictures.

The experiments were configured to observe the structure in the free shear layer, so the images were further magnified and only the portion of the line passing through the free shear layer was observed. Measurement locations 1.04 cm downstream of the nozzle (2.2 mm before the Mach disk) and 1.35 cm downstream of the nozzle (.9 mm after the Mach disk) were

chosen. Figure 5 shows a composite image of a displaced line across the free shear layer at the first measurement station superimposed on the recorded baseline. By carefully measuring the displacement, the centerline velocities at the two measurement locations were found to be 598 ± 20 m/s, and 112 ± 20 m/s, respectively. As indicated in Table I, the first measurement is in excellent agreement with the calculated value, and the second measurement is somewhat lower than the calculated value. The major contribution to the velocity uncertainty is the measurement of the distance the line has moved. For example, the distance moved for the centerline measurement downstream of the Mach disk is 230 microns. The resolution of the camera is 16.6 microns/pixel, so a one-pixel error in the measurement corresponds to 8.3 m/s. Higher accuracy can be achieved by a higher resolution camera or a longer time interval between tagging and interrogation.

Figure 6 shows a composite of close-up pictures of lines across the free shear layer at the first measurement location. A far-UV filter was placed over the camera so density information (Rayleigh scattering) has been eliminated to simplify the data reduction. Figure 7 shows a similar composite image taken at the second measurement location, downstream of the Mach disk. The images on these figures were preselected to show examples of large-scale structural features. Figures 8 and 9 are composite images which have been preselected to show examples of intermediate-scale structural features.

Figures 10 and 11 show the computed statistics from the recorded line

images. In these figures the top curve is the average velocity profile, $u(x)$; the second curve is the turbulence intensity, $(\overline{u^2})^{1/2}$; and the bottom curve shows the correlation of the velocity with the value at the center of the free shear layer. Figure 10 was constructed from 50 images recorded at the first measurement location, and Fig. 11 was constructed from 70 images recorded at the second measurement location. It is important to note that the sampling rate was slow enough that there is no time correlation between separate recorded line images. Both the broad correlation function and the individual line profiles shown in Figs. 6 and 7 indicate the presence of large-scale coherent structures. This is consistent with the observation of Lepicovsky et al. (13), who used schlieren and laser velocimetry in a Mach 1.4 supersonic jet.

For future work, the RELIEF tagging method can be extended to simultaneously mark several lines, or to multiply interrogate a single line at several time intervals. Since tagging is accomplished by overlapping two lasers, single points or multi-dimensional arrays of points can be marked to permit a three-dimensional measurement of velocity, vorticity, and shear stress.

ACKNOWLEDGMENTS

This work was supported by the U.S. Air Force Office of Scientific Research under Grants AFOSR 86-0191 and AFOSR 86-0219.

REFERENCES

1. R. Miles, C. Cohen, J. Connors, P. Howard, S. Huang, E. Markovitz, and G. Russell, Optics Letters 12, 861 (1987).
2. L.J. Lu and C.R. Smith, "Image Processing of Hydrogen Bubble Flow Visualization for Determination of Turbulence Statistics and Bursting Characteristics," Experiments in Fluids 3, 349-356 (1985).
3. E. Mach and P. Salcher, Wien. Ber 98, 1303 (1889).
4. L. Prandtl, Physik Zeits 5, 599 (1904).
5. R. Ladenburg, C.C. Van Voorhis, and J. Winckler, Physical Review 76, 662 (1949).
6. M.L. Norman, L. Smarr, K.-H.A. Winkler, and M.D. Smith, Astron. Astrophys. 113, 285 (1982).
7. S.M. Dash, H.S. Pergament, D.E. Wolf, N. Sinha, M.W. Taylor, "JANNAF Standard Plume Flow Field Mode (SPF 2)," Vol. II, SAI/PR TR-18-II, (May 1984).

8. M. Zimmermann, S. Cheng, and R.B. Miles, "Measurements of Supersonic Nitrogen Flow Properties with the Resonant Doppler Velocimeter," 1981 IEEE/OSA Conference on Lasers and Electro-Optics, Washington, D.C., June 1981, CLEO'81 Technical Digest, Paper W02, Washington D.C., Optical Society of America, 1980, page 62.
9. K. Grywatz, M. Reich, V. Zobel, U. Brinkmann, and J. Kluge, *Laser und Electro-Optik* 4, 6 (1981).
10. J.C. McDaniel, D. Baganoff, and R.L. Byer, *Phys. of Fluids* 25, 1105 (1982).
11. M. Zimmerman, S. Cheng, and R.B. Miles, "Flow Visualization in Supersonic Air with the Resonant Doppler Velocimeter," Phoenix, AZ, 1982, CLEO'82 Technical Digest, Paper ThS4, Washington, D.C.: Optical Society of America, 1982.
12. R. Frey, J. Lukasik, and J. Ducuing, *Chem. Phys. Lett.* 14, 514 (1972).
13. J. Lepicovsky, K.K. Ahuja, W.H. Brown, and R.H. Burrin, "Coherent Large-Scale Structures in High Reynolds Number Supersonic Jets," *AIAA Journal* 25, 1419 (1987).

TABLE I

CENTERLINE PARAMETERS (CALCULATED) (7)

$P_o = 1.03 \times 10^6$ pascal (150 psia), $T_o = 250$ K,
 $P_{\text{ambient}} = 1.01 \times 10^5$ pascal (14.7 psia),
 Exit Diameter = 6.35 mm (.25")

	LOCATION (mm)	VELOCITY (m/sec)	PRESSURE (pascal)	TEMP. (K)	MACH #	DENSITY g/cc
	.127	292	5.40×10^5	208	1.01	.00906
	2.69	433	2.02×10^5	157	1.72	.00449
	5.23	529	5.95×10^5	111	2.51	.00187
	7.80	576	2.33×10^4	85	3.13	.00096
MEASUREMENT LOCATION--	10.3	604	1.12×10^4	68	3.64	.00057
MACH DISK-----	12.6	621	6.27×10^3	58	4.06	.00038
MEASUREMENT LOCATION--	13.5	134	1.06×10^5	241	.43	.00153

FIGURE CAPTIONS

Figure 1. Structure of an underexpanded sonic jet.

Figure 2. Experimental layout.

Figure 3. Orthographic projection of the test region.

Figs. 4a-d. Density cross sections of an underexpanded sonic jet with lines tagged before and after the Mach disk. (The round feature at the bottom is an artifact due to strong light scattering off the nozzle face.) Flow is from bottom to top.

Figure 5. Composite image of a displaced line across the free shear layer 2.2 mm before the Mach disk superimposed on an undisplaced baseline. Flow is from bottom to top. Maximum displacement is 1.19 mm, and the time interval is $2\mu\text{sec}$.

Figure 6. Composite picture of four separate recorded images of lines across the free shear layer 2.2 mm before the Mach disk. The images have been selected to show large-scale structure.

Figure 7. Composite picture of four separate recorded images of lines across the free shear layer .9 mm after the Mach disk. The images have been selected to show large-scale structure.

Figure 8. Composite picture of four separate recorded images of lines across the free shear layer 2.2 mm before the Mach disk. The images have been selected to show intermediate-scale structure.

Figure 9. Composite picture of four separate recorded images of lines across the free shear layer .9 mm after the Mach disk. The images have been selected to show intermediate scale-structure.

Figure 10. Measured velocity, turbulence intensity, and correlation function 2.2 mm upstream of the Mach disk.

Figure 11. Measured velocity, turbulence intensity, and correlation function .9 mm downstream of the Mach disk.

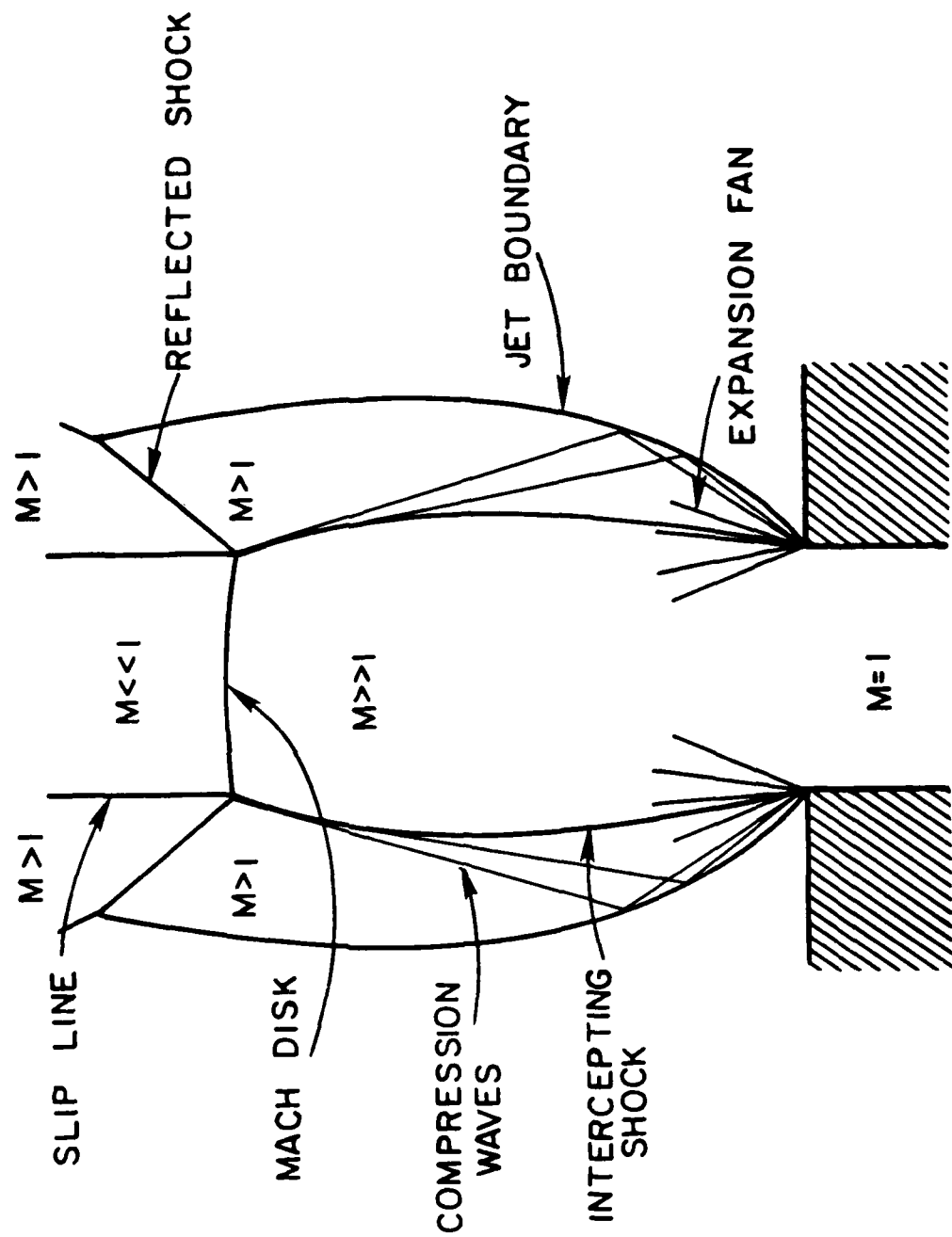


Figure I

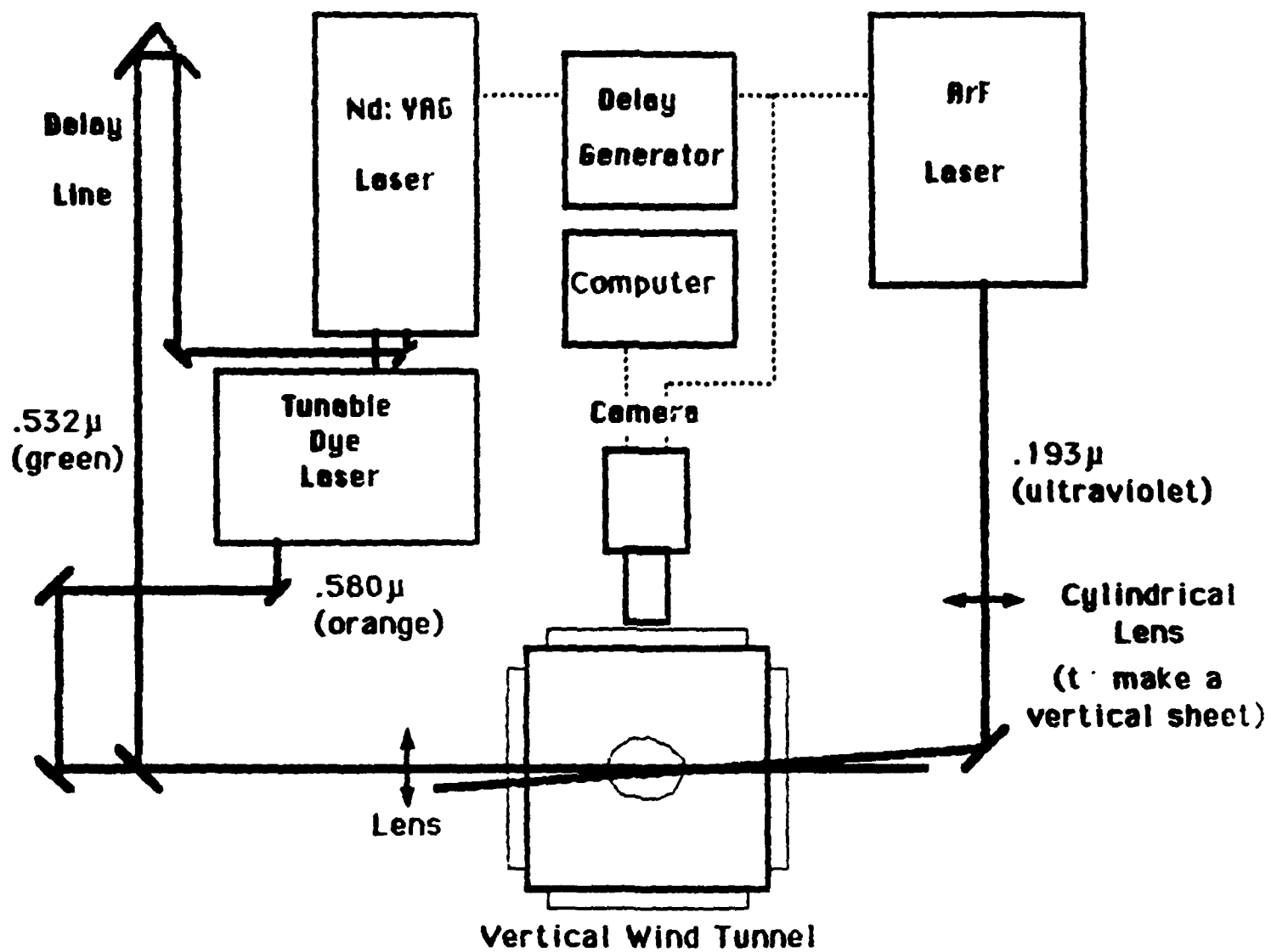


Figure 2

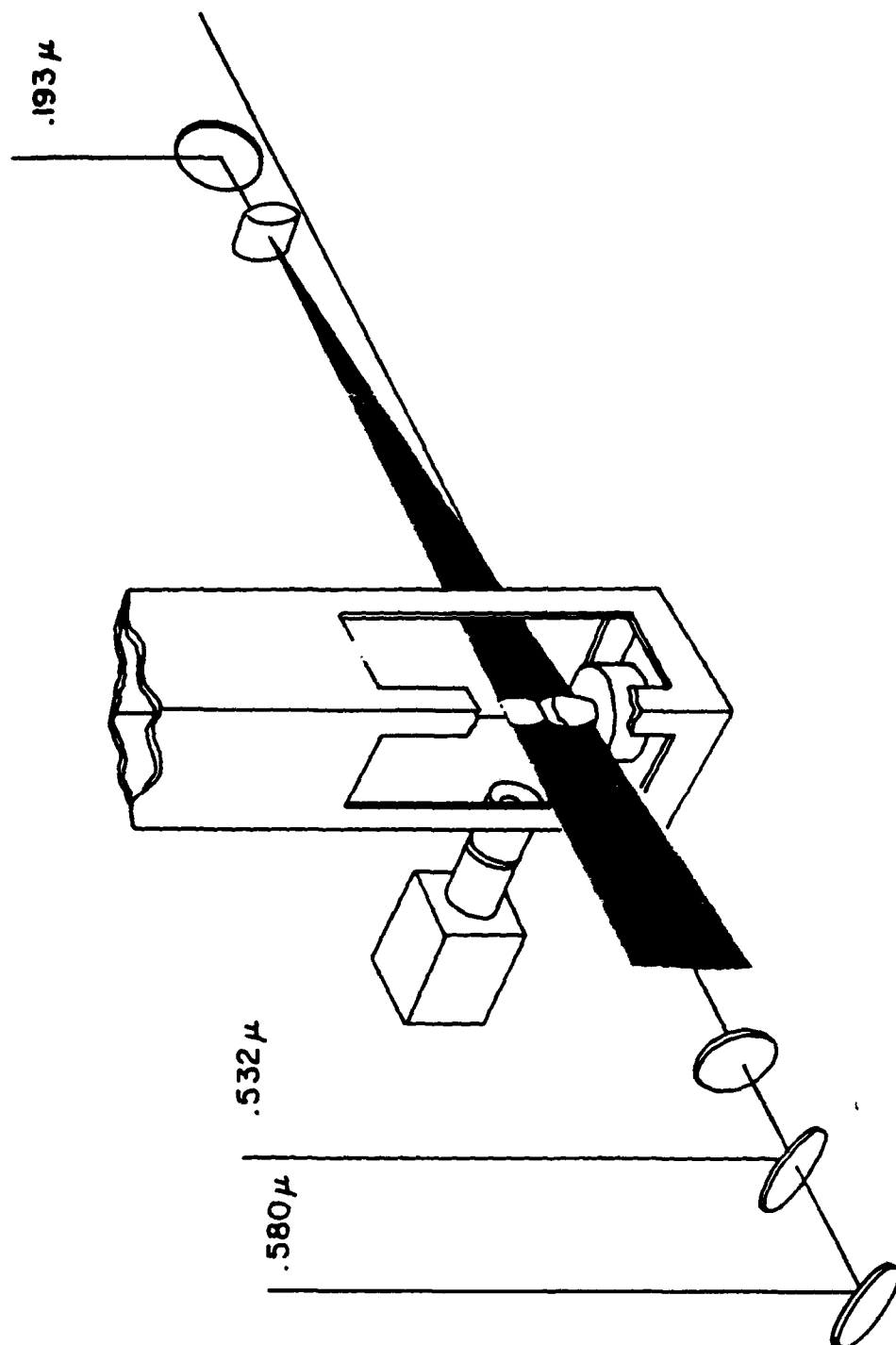
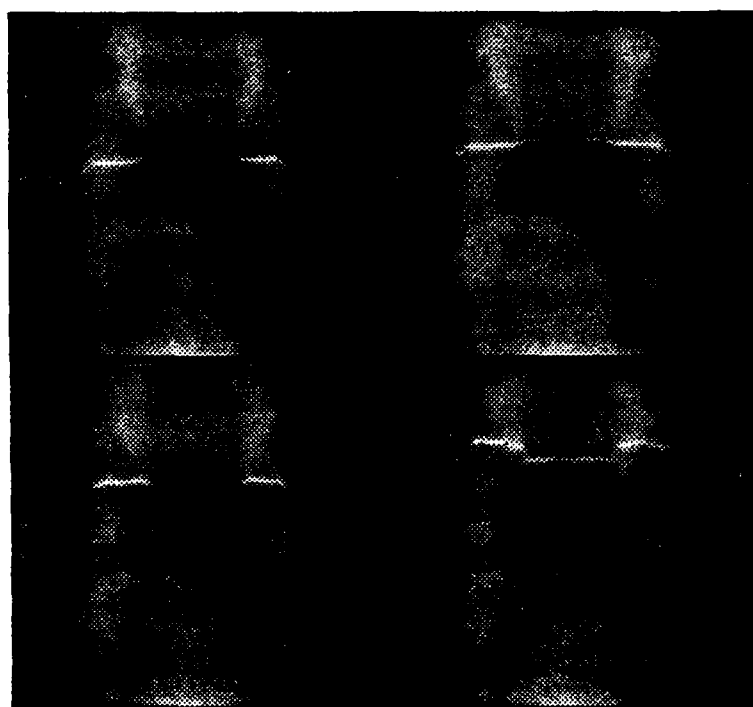


Figure 3

4a

4b



4c

4d

Fig. 4a-4d

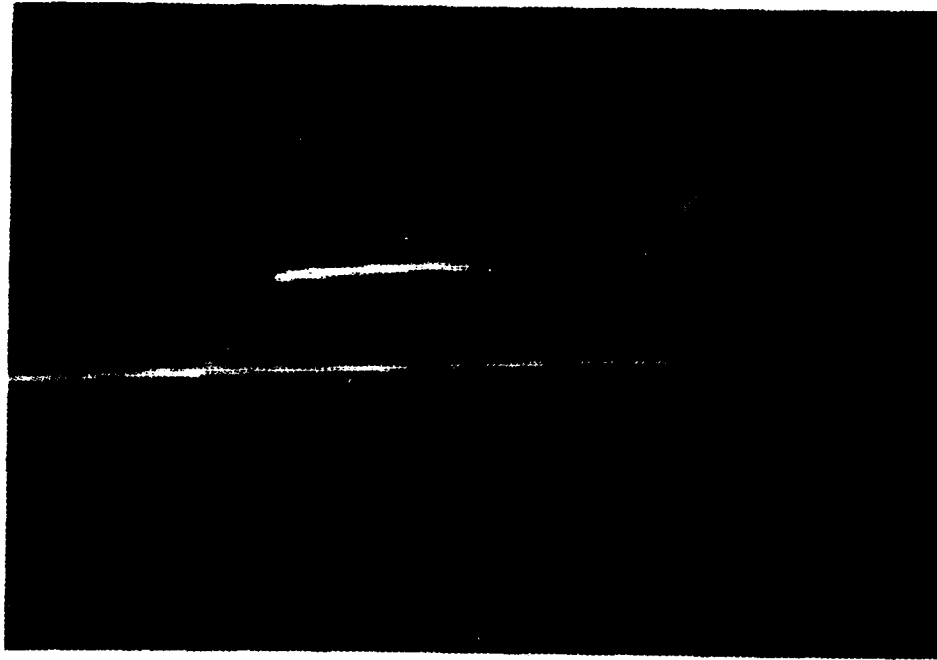


Figure 5

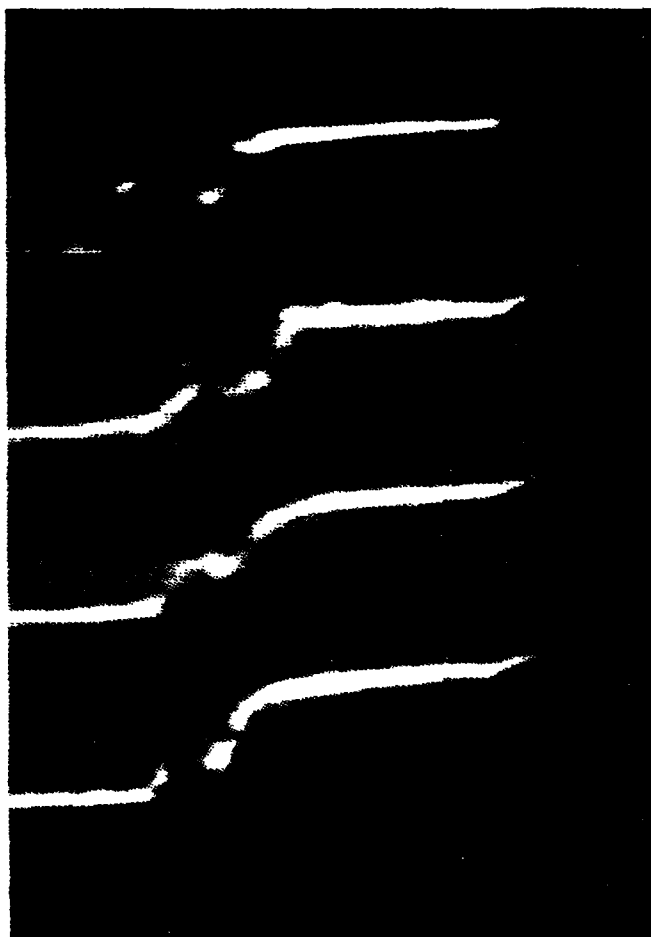


Figure 6

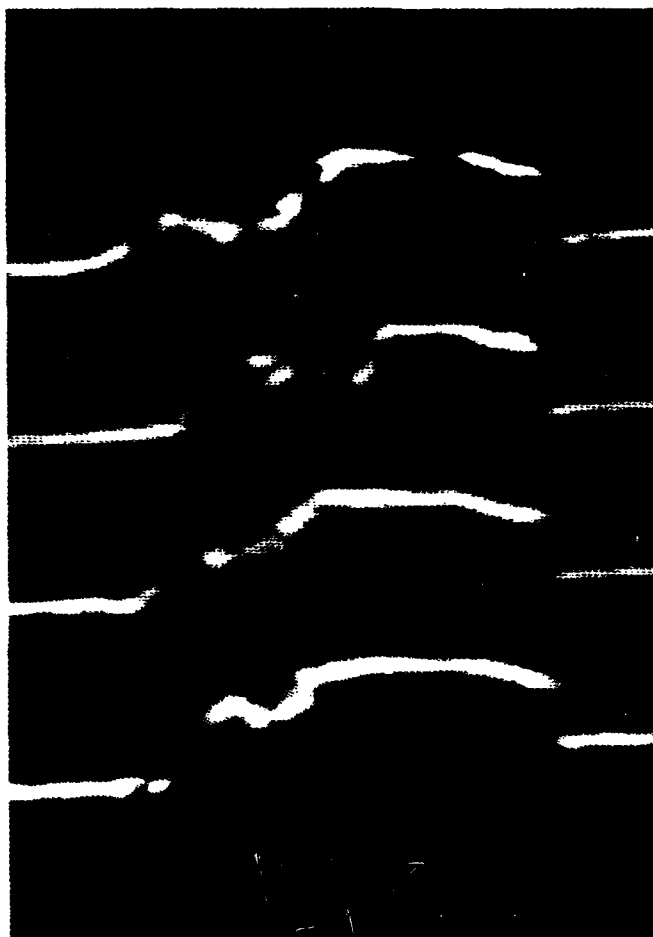


Figure 7



Figure 8

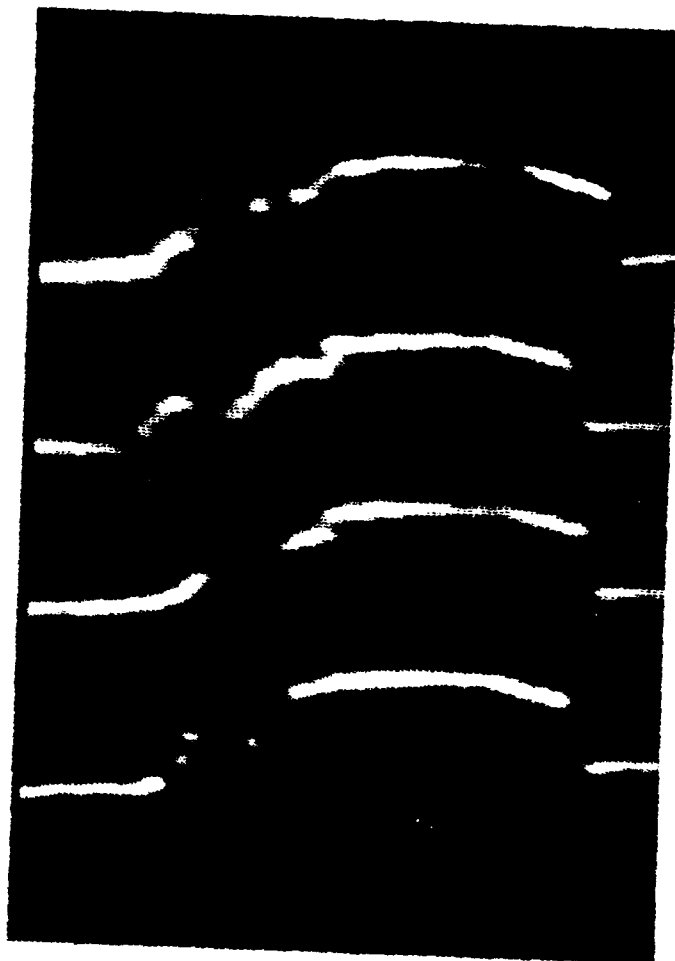


Figure 9

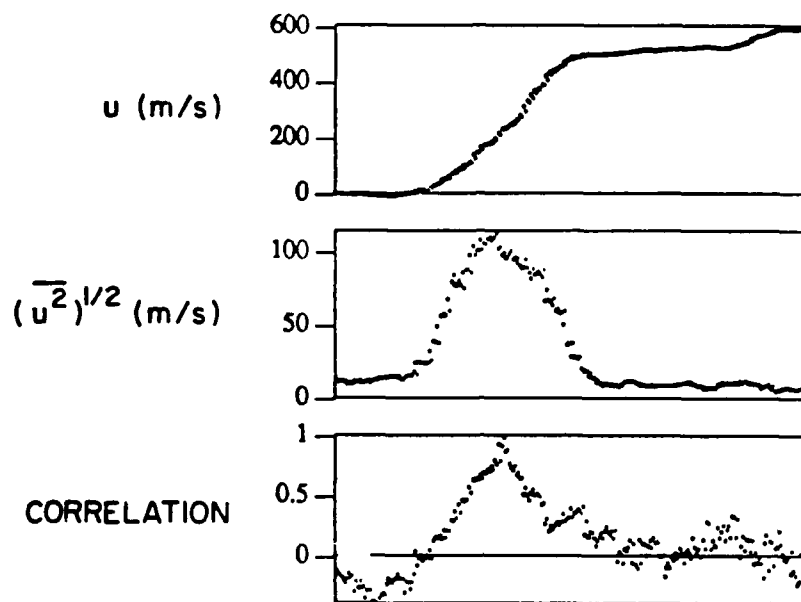


Figure 10

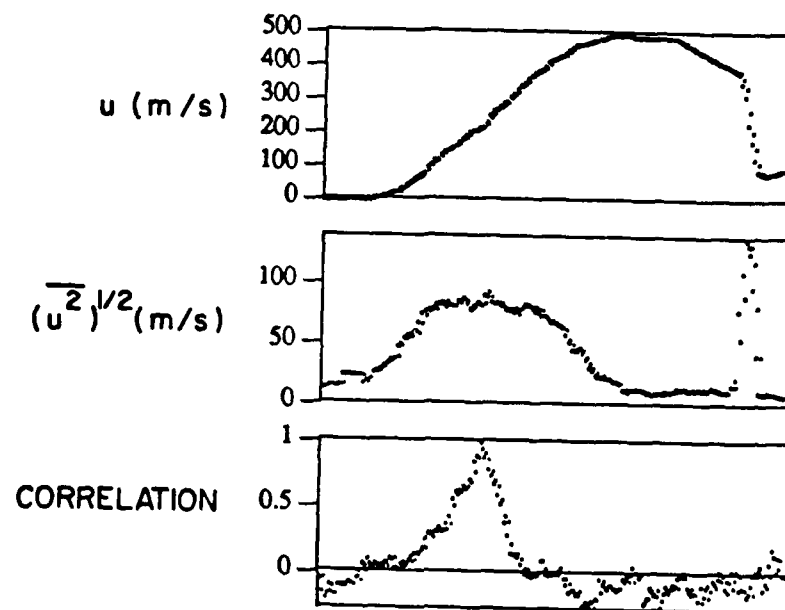


Figure 11

INSTANTANEOUS PROFILES AND TURBULENCE STATISTICS
OF SUPERSONIC FREE SHEAR LAYERS BY RAMAN EXCITATION +
LASER-INDUCED ELECTRONIC FLUORESCENCE (RELIEF)
VELOCITY TAGGING OF OXYGEN

R.B. Miles, J.J. Connors, E.C. Markovitz,
P.J. Howard, and G.J. Roth

Department of Mechanical & Aerospace Engineering
PRINCETON UNIVERSITY
Princeton, New Jersey 08544 U.S.A.

Abstract.

A new method of flow tagging based on the vibrational excitation of oxygen is applied to both supersonic and high-speed subsonic air flows to generate instantaneous velocity profiles and turbulence statistics across the free shear layer.

By simultaneously tagging two lines, both transverse and streamwise velocity correlations are found. Rayleigh scattering can also be imaged, so this flow diagnostic technique has the capability of instantaneously recording density cross sections and velocity profiles.

1 Introduction

Our understanding of the fundamental properties of turbulence in high-speed flows has been limited by the lack of experimental techniques capable of generating instantaneous multipoint data. In shear layers, turbulent structures and the evolution of these structures play a critical role in heat transfer, drag, and mixing. Previous measurement techniques have relied largely on hot wire probes, laser doppler velocimetry, and schlieren to infer the properties of turbulent structures. Such fundamental questions as the velocity at which these structures move, the scale of the structures, their form, and the corresponding vorticity fields are unresolved.

This paper outlines a new measurement technique in which lines are instantaneously written into high-speed air and their

displacement after a well defined time intervals is recorded. In essence, this technique introduces to the compressible gas community a tool which is similar to the hydrogen bubble flow marking capability which has been so important in water channels (Lu and Smith 1985). Our technique has been applied in both the low-speed and the high-speed flow regimes and requires no seeding since the tracking is done with molecular oxygen. The results presented in this paper show both instantaneous and time-averaged velocities plus turbulence statistics across a Mach 3.6 free shear layer in an axisymmetric free air jet. These results are presented together with subsonic measurements to elucidate the difference between supersonic and subsonic turbulence.

2 Background discussion

The method which is used to tag and follow the flow is a combination of Raman Excitation + Laser-Induced Electronic Fluorescence (RELIEF) (Miles et al. 1987). It is made possible by the fact that oxygen in its vibrationally excited state has an exceptionally long lifetime (Frey et al. 1972). Consequently, the flow can be tagged by vibrationally exciting oxygen molecules at a specific point or in a line at a given instant in time. At a later instant in time, these molecules are further excited to an electronic state which fluoresces. The fluorescence is recorded on a high-sensitivity camera and the corresponding point displacement or line profile gives a quantitative measure of the velocity and the flow structure.

Oxygen is a homonuclear diatomic molecule and therefore has no dipole moment. This is responsible for its long vibrational lifetime, but also means that vibrational excitation by the absorption of a single photon is not possible. Consequently, one must use a two-photon process called stimulated Raman scattering to vibrationally excite the molecules. This is done by simultaneously using two lasers which differ in frequency by the vibrational frequency of oxygen. Since stimulated Raman scattering is a nonlinear process, both lasers must be very high intensity to drive a significant number of molecules into the vibrationally excited state. Practically, the intensity is limited by the breakdown threshold of air.

In our experiments, a high-powered Nd:YAG laser and a Nd:YAG pumped dye laser were used to simultaneously generate beams at .532 micrometers (green) and .580 micrometers (orange). The pulses were 10 nsec in duration and were synchronized in time such that they passed through the tagging volume simultaneously. The maximum energy of these lasers at the test section was 50 mJ and 40 mJ, respectively, and they were focused to a beam diameter of approximately 50 micrometers measured between the e^{-2} intensity points of the Gaussian shaped beams. This resulted in maximum power densities on the order of 500 GW/cm², well in excess of what is required to saturate the transition (Miles et al. 1988), and somewhat higher than the breakdown threshold of air in a static cell. Good flow marking could be seen at considerably lower intensities, but the lasers were operated at the highest intensities possible to optimize the signal-to-noise. The oxygen transitions which are driven with this pair of lasers correspond to the Q-branch, or those transitions in which the initial and final rotational states are identical. As a consequence, the cooling of the ground state due to the removal of molecules is just offset by the heating of the excited state, so the tagging mechanism leaves the temperature virtually unchanged. The rotational levels of both the ground state and the vibrationally excited state reach thermal

equilibrium in a few collisions.

The dye laser is tuned to access the most highly populated rotational state in order to get the largest number of molecules possible into the vibrationally excited state. A plot of the 300 K vibrational excitation versus the frequency difference of the two lasers is shown in Fig. 1. Since the lasers are very narrow linewidth (the Nd:YAG laser is injection-locked), the detailed line structure of the rotational states is apparent. For flow tagging, the difference in laser frequencies is selected to correspond to the highest peak in Fig. 1. It is interesting to note that by tuning the dye laser continuously, the rotational populations can be measured which, in turn, give the temperature. Consequently, this technique may also be used to generate a time-averaged temperature profile of the flow field. The bottom curve is the rotational spectrum calculated for 300 K.

The fact that two lasers must be used to tag the oxygen is a benefit since tagging only occurs where they overlap. In the experiments discussed here, the beams have been made colinear to mark lines in the flow. In general, however, they may be crossed to mark points, crossed at an angle to mark short line segments for vorticity measurements, or multiplicity crossed to mark two- or three-dimensional grids. Since very little of the laser light is lost in the pumping process, the lasers may be reflected back and forth through the flow to simultaneously mark additional lines.

The interrogation step is accomplished with a narrow linewidth ultraviolet ArF excimer laser which further excites the vibrationally excited molecules up to the $v'=7$ state in the oxygen Schumann-Runge band. Figure 2 shows the tuning range of the ArF laser and the various lines associated with transitions from the ground and first vibrational state of oxygen which fall within that range. The ArF laser is generally tuned to the P(19) or R(21) lines or the P(23) or R(25) lines of the $v'=7$, $v''=1$ manifold. The P(21) and R(23) lines of that manifold fall on top of absorption lines from the ground state of oxygen and are, consequently, avoided. In fact,

transitions from ground state oxygen are not seen because the oxygen in the laser cavity itself and in the air path between the laser and the test cell absorbs those photons. The $v'-7$ state of the Schumann-Runge band is strongly predissociated so that most of the oxygen molecules excited to that state break apart into oxygen atoms. Only one part in 10^5 of these molecules fluoresce, so the image must be recorded with a high-sensitivity camera. The fluorescence yield is further reduced by the poor Franck-Condon coupling factor between the $v'-7$ and $v"-1$ states, and the fact that only very few of the molecules in the vibrationally excited state lie in the high rotational states which can be accessed by the ArF laser. By choosing other (more complex) ultraviolet lasers, signal enhancements on the order of 1,000 or more can be expected. Nevertheless, interrogated lines are readily visible with the ArF laser, as will be seen later.

The ArF laser generates a large amount of Rayleigh scattering which may be simultaneously imaged to give the density. In our experiments, the ArF laser was loosely focused to a sheet which intersected the flow longitudinally. This sheet was several hundred microns thick so that the tagged molecules would stay inside the ArF illumination region during the time intervals of interest. If no far UV-blocking filter was used, the Rayleigh scattering was simultaneously collected giving a qualitative picture of the density simultaneous with the line interrogation. When the velocity data was taken, a UV-blocking filter was placed in front of the camera so that only the tagged line was seen.

3 Computer data analysis system

Images were acquired at the 10 Hz repetition rate of the laser systems and were downloaded from the video camera to a frame grabber and then either read directly into the computer or stored on videotape. The videotape provided a permanent record and, in most cases, computer processing was done offline by reading the videotape. A computer program was written which could extract a small rectangular window from each image and

rapidly transfer that data into the memory of the SUN 3/160 computer. The window was selected to include that portion of the line of interest. In the cases where two lines were simultaneously marked, the window was expanded to include both lines. After the data was loaded into the computer, the location of the lines was determined by searching for the brightest pixels in each subsequent vertical row of pixels while stepping through each image window from left to right. The search was weighted towards the point located in the previous vertical row of pixels to favor continuity of the line. This allowed multiple lines to be tracked on the same image and eliminated random jumps to bright noise spots far from the tagged line. The center of the line was determined using a weighted sum of the pixels surrounding the brightest pixel.

Following line identification, the image windows were displayed by the computer with the identified line location shown superimposed on the original data. Each individual image was reviewed to be sure that the line or lines identified did, in fact, lie on top of the recorded lines in the image. If not, that particular image window was deleted. When the final set of images was selected, the computer found the average velocity profiles and the turbulence intensity. Following that, any point across the velocity profile could be selected and the computer presented a histogram of the velocity values at that point and correlations of the u component of the velocity at that point with the u component of the velocities at the other points across the velocity profile. For the cases where two lines were marked, the computer also generated the correlation of the velocity across the other line with the selected velocity component.

4 Velocity profiles across a supersonic jet

A versatile axisymmetric free jet facility was constructed to provide a test environment for the development of the RELIEF technique. For the high-speed measurements a sonic orifice was used to generate an underexpanded free jet. The plenum was operated at 150 psia and reached an

equilibrium temperature of 250 K. The jet exited into a 1 atm test chamber through a 6.35 mm (.25") diameter nozzle. The Reynolds number was approximately 1.2×10^6 based on the exit diameter. An orthographic projection of the test chamber plus the laser beams and camera system is shown in Fig. 3. The tagging beams were focused into the chamber from the left and were reflected back with a mirror so that two lines were simultaneously tagged. The separation between these two lines could be arbitrarily selected. The ArF laser passed through a cylindrical lens and was focused to a sheet of light which entered the chamber from the right. A gated and intensified CID videocamera recorded both the Rayleigh scattering from the air and the laser-induced electronic fluorescence from the tagged oxygen molecules.

A diagram of the structure of an underexpanded supersonic free jet is shown in Fig. 4. That structure is echoed in the photograph shown in Figs. 5 and 6 where a line has been marked upstream and downstream of the Mach disk respectively in the figures, and the far UV filter has been left off the camera to allow scattering to simultaneously be imaged. In each figure the line was straight when tagged, so the deformation of the line is a quantitative measure of the instantaneous velocity profile. The image was recorded with a single interrogation pulse, approximately 2 microseconds after the line was tagged.

The Rayleigh scattering gives a qualitative view of the shock structure, the free shear layer, and the density variations. Since the interrogation laser is only on for 10 nanoseconds, all of the unsteady phenomenon are frozen. The tagged lines give a quantitative measure of the velocity profile upstream and downstream of the Mach disk. The most notable features are the large discontinuities across the slip lines downstream of the Mach disk. Turbulent structure in the free shear layer can also be seen in both images, and outside of the jet the flow is so slow that virtually no displacement of the line has occurred during the 2 microsecond interval.

A computational model was run (Dash et al., 1984) which was matched to the operating conditions of our jet. Table I gives the computed centerline values for the velocity, Mach number, temperature, density, and pressure. Centerline measurements were made upstream and downstream of the Mach disk as indicated in the Table, yielding measured velocities of 598 ± 20 m/s and 112 ± 20 m/s, respectively. The upstream value is in close agreement with the computed value of 604 m/s, but the downstream measurement is significantly lower than the computed value of 134 m/s. Experimental errors in the velocity measurement are largely due to errors both in calibrating the displacement and measuring the line positions. The camera resolution in the downstream direction is 16.6 microns/pixel, so a 1 pixel error is equivalent to 8 m/s.

We were particularly interested in the characteristics of the turbulence across the free shear layer. Simultaneous two-line flow marking was done with a line separation of .76 mm so that velocity correlations in the streamwise direction could be examined. The line positions were approximately 11.2 mm and 11.9 mm from the nozzle exit. The camera and lens were positioned so close-up images across the free shear layer could be observed. The flow was sampled 1 microsecond after tagging and an example of 8 separate line pairs is shown in Fig. 7. The flow is from bottom to top and the high-speed region is at the left in each image. Approximately 100 such images were used to calculate the average velocity profiles and turbulence intensities associated with the two lines. These are shown in Figs. 8a and 8b and 9a and 9b for the upstream and downstream location respectively. Figures 8c and 9c show the correlations of the measured velocities across the free shear layer with the velocity at the point where the mean velocity has fallen to one-half of the maximum.

The velocities could also be correlated between the two simultaneously tagged lines. Figures 10a to 10d show expanded views of these correlations taken from 140 double line images. Figure 10a shows the correlation of the velocities across the downstream line with the

downstream velocity at the half maximum point. Figure 10b shows the correlations of the velocities in the upstream line with the downstream velocity selected at the same point. Similarly, Fig. 10c shows the correlations of the upstream velocities across the shear layer with the upstream velocity at the half maximum velocity point. Figure 10d shows the correlation of the downstream velocities with the upstream velocity selected at the same point.

5 Flow tagging across a low-speed jet

A comparison between subsonic and supersonic flows can be made running the same facility at a lower plenum pressure. In this case the plenum pressure was dropped to 23 psia and the plenum temperature stabilized at 293 K. The tagged lines were separated by .74 mm and the downstream line was 12.2 mm from the nozzle exit. The Reynolds number of the jet was approximately 3×10^4 and the time between tagging and interrogation was 2 microseconds. The centerline velocity was measured to be 273 m/s. A collage of six image windows taken with simultaneous two-line marking across this subsonic jet is shown in Fig. 11. In this case the bright pixels indicating the computer-identified lines are shown superimposed on the data. Once again, the computer calculated the average velocity, the turbulence intensity, and the correlation across the free shear layer as shown in Figs. 12a to 12c and 13a to 13c for the upstream and downstream lines, respectively. Correlations done in a manner similar to those in the supersonic flow are shown in Figs. 14a to 14d.

A comparison of the supersonic and subsonic flows leads to the following observations:

- 1) The supersonic turbulence intensity appears skewed toward the outer portion of the free shear layer.
- 2) The supersonic velocity appears to be correlated over a larger fraction of the free shear layer than does the subsonic velocity.

Since only on the order of 100 images (limited by the memory of the computer) were sampled to generate the statistics, these observations are tentative.

6 Summary

The RELIEF method for tagging both high-speed and low-speed air shows great promise for enhancing our understanding of turbulence. Lines can be instantaneously marked and followed in air flows in much the same manner that hydrogen bubble lines can be tracked in water. In this paper the results of preliminary experiments across the free shear layer of an underexpanded sonic jet have been presented. A comparison with a subsonic jet suggests that there is a reduced growth rate of the free shear layer of the supersonic flow. Further experiments using the RELIEF technique to tag multiple points for three-dimensional velocity field measurements, and small line segments for vorticity measurements will further elucidate the characteristics of turbulence both in the high-speed and low-speed regimes.

ACKNOWLEDGEMENT

This work was supported by the U.S. Air Force Office of Scientific Research under Grant Number AFOSR 86-0191. The authors would also like to acknowledge helpful comments from Alexander Smits and Forman Williams.

REFERENCES

- Dash, S., Pergament, H., Wolf, D., Sinha, N., and Taylor, M. 1984: JANNAF Standard Plume Flow Field Mode (SPF 2) Vol. II, SAI/PR TR-18-II.
- Frey, R., Lukasik, J., and Ducuing, J. 1972: Tunable Raman Excitation and Vibrational Relaxation in Diatomic Molecules. *Chemical Physics Letters* 14, 514-517.
- Lu, L., Smith, C. 1985: Image Processing of Hydrogen Bubble Flow Visualization for Determination of Turbulence Statistics and Bursting Characteristics. *Experiments in Fluids* 3, 349-356.
- Miles, R., Cohen, C., Connors, J., Howard, P., Huang, S., Markovitz, E., and Russell, G. 1987: Velocity Measurements by Vibrational Tagging and Fluorescent Probing of Oxygen. *Optics Letters* 12, 861.
- Miles, R., Connors, J., Markovitz, E., and Roth, G. 1988: Coherent Anti-Stokes Raman Scattering (CARS) and Raman Pumping Lineshapes in High Fields. (to be published in SPIE Conference Proceedings). SPIE Meeting, Los Angeles, CA, January 11-15, 1988.

TABLE 1
CENTERLINE PARAMETERS (CALCULATED)
(Dash et al. 1984)

$P_0 = 1.03 \times 10^6$ pascal (150 psia), $T_0 = 250$ K.
 $P_{\text{ambient}} = 1.01 \times 10^5$ pascal (14.7 psia).
Exit Diameter = 6.35 mm (.25")

LOCATION (mm)	VELOCITY (m/sec)	PRESSURE (pascal)	TEMP. (K)	MACH #	DENSITY g/cc
.127	292	5.40×10^5	206	1.01	.00906
2.69	433	2.02×10^5	157	1.72	.00449
5.23	529	5.95×10^5	111	2.51	.00187
7.80	576	2.33×10^4	85	3.13	.00096
MEASUREMENT LOCATION--10.3	604	1.12×10^4	68	3.64	.00057
MACH DISK-----12.6	621	6.27×10^3	58	4.06	.00038
MEASUREMENT LOCATION--13.5	134	1.06×10^5	241	.43	.00153

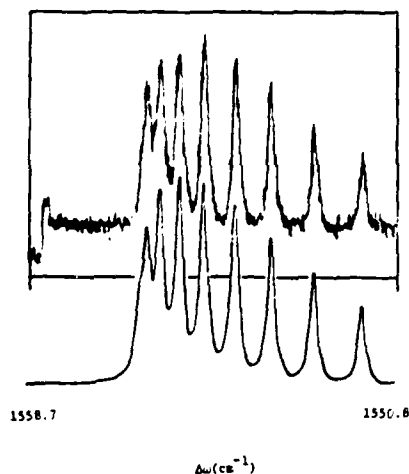


FIG. 1. ROTATIONAL STRUCTURE OF THE $v''=0$ TO $v''=1$ STIMULATED RAMAN TRANSITION AT 300 K. THE UPPER CURVE IS MEASURED AND THE LOWER CURVE IS CALCULATED.

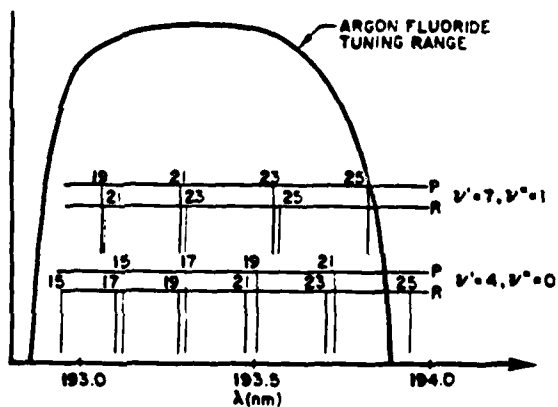


FIG. 2. OVERLAP OF THE ArF-LASER TUNING CURVE WITH THE TRANSITIONS FROM THE GROUND ($v''=0$) AND VIBRATIONALLY EXCITED ($v''=1$) STATES OF OXYGEN.

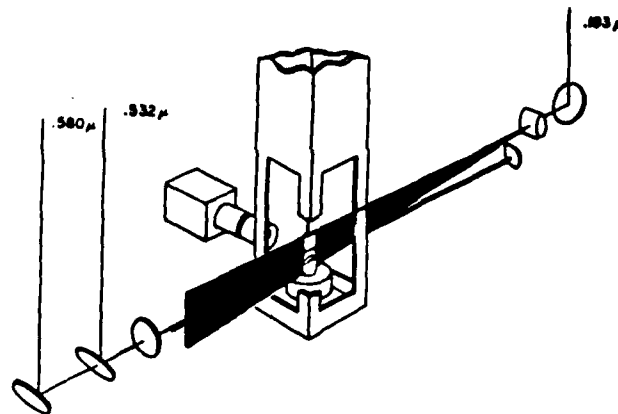


FIG. 3. ORTHOGRAPHIC PROJECTION OF THE TEST REGION.

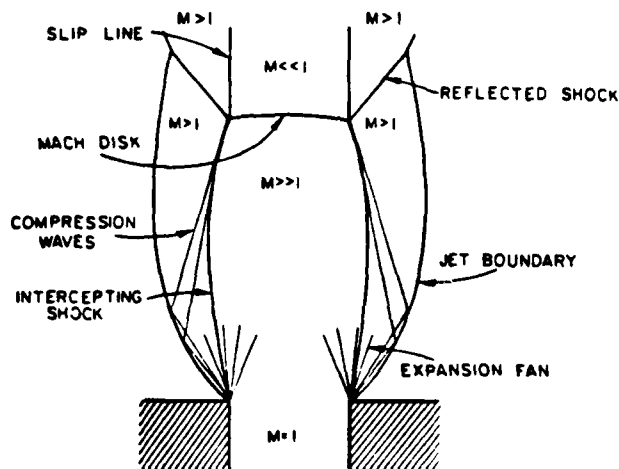


FIG. 4. STRUCTURE OF AN UNDEREXPANDED SONIC JET.

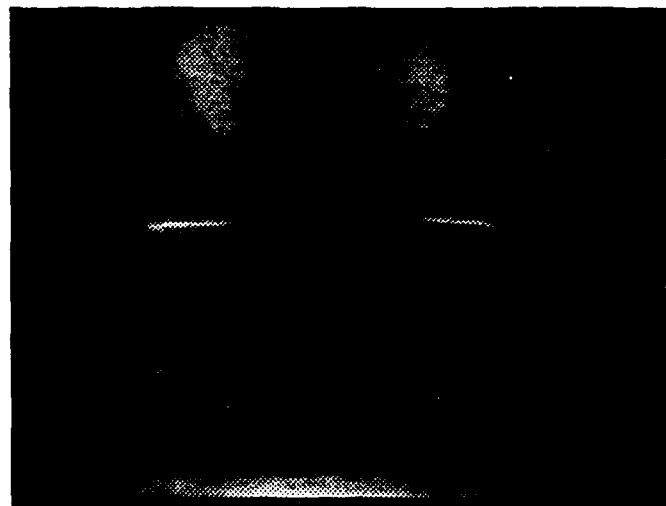


FIG. 5. CROSS SECTION OF UNDEREXPANDED JET WITH A LINE MARKED UPSTREAM OF THE MACH DISK. THE LINE WAS STRAIGHT WHEN MARKED, SO THE DISPLACEMENT IS A QUANTITATIVE MEASURE OF THE VELOCITY PROFILE. RAYLEIGH SCATTERING IS IMAGED TO GENERATE THE DENSITY (THE ROUND FEATURE AT THE BOTTOM IS AN ARTIFACT DUE TO LIGHT SCATTERING).

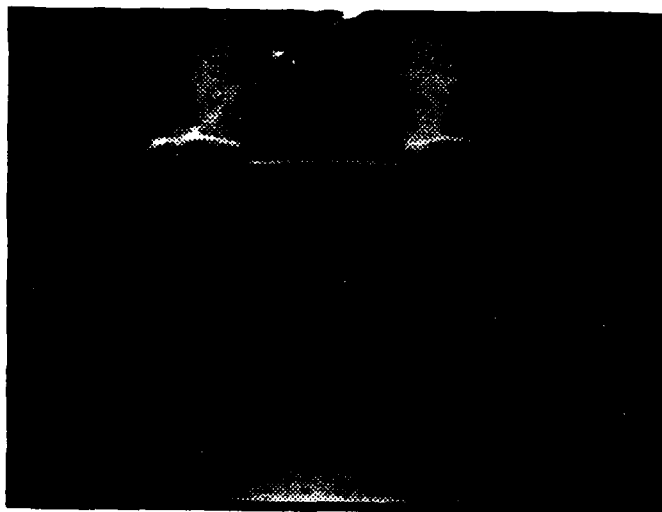


FIG. 6. CROSS SECTION OF UNDEREXPANDED JET WITH A LINE MARKED DOWNSTREAM OF THE MACH DISK. THE LINE WAS STRAIGHT WHEN MARKED, SO THE DISPLACEMENT IS A QUANTITATIVE MEASURE OF THE VELOCITY PROFILE. RAYLEIGH SCATTERING IS IMAGED TO GENERATE THE DENSITY (THE ROUND FEATURE AT THE BOTTOM IS AN ARTIFACT DUE TO LIGHT SCATTERING).

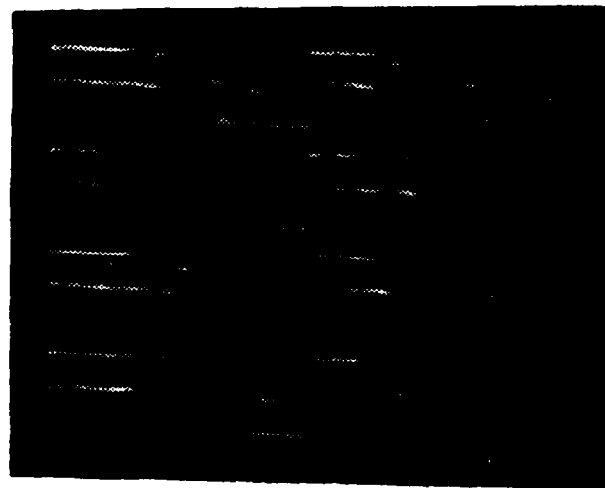


FIG. 7. TAGGED LINE PAIRS ACROSS A SUPERSONIC FREE SHEAR LAYER.

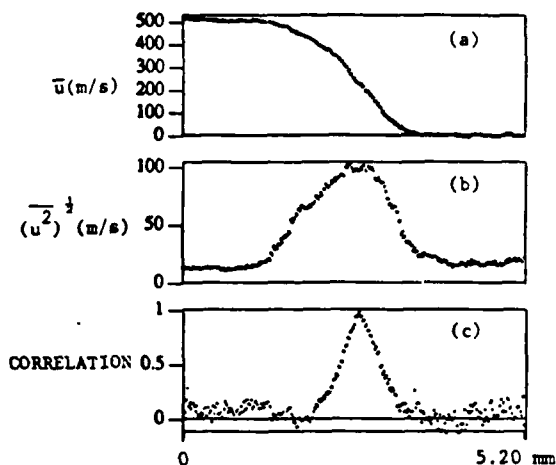


FIG. 8. (a) AVERAGE VELOCITY, (b) TURBULENCE INTENSITY, AND (c) VELOCITY CORRELATION ACROSS A SUPERSONIC FREE SHEAR LAYER 11.2 mm DOWNSTREAM OF THE NOZZLE EXIT.

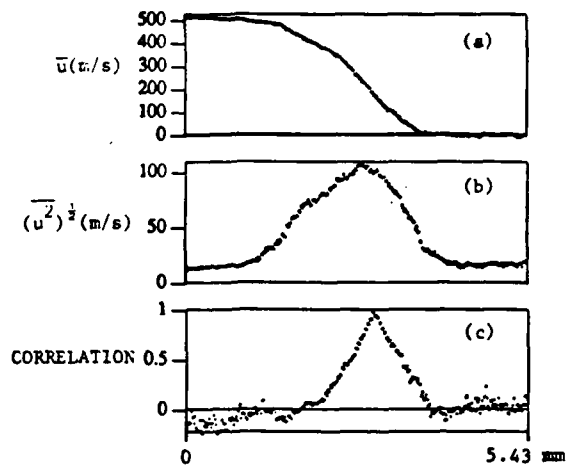


FIG. 9. (a) AVERAGE VELOCITY, (b) TURBULENCE INTENSITY, AND (c) VELOCITY CORRELATION ACROSS A SUPERSONIC FREE SHEAR LAYER 11.9 mm DOWNSTREAM OF THE NOZZLE EXIT.

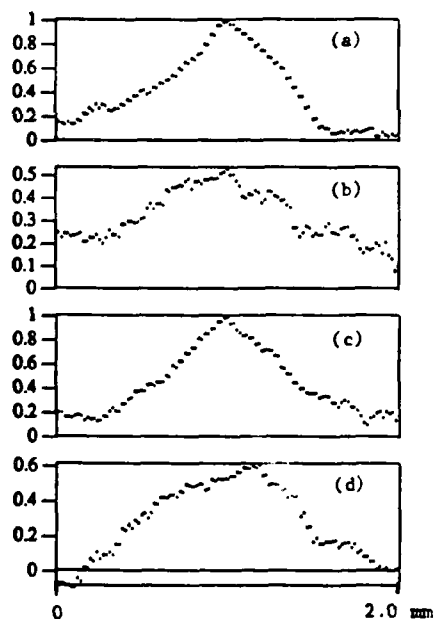


FIG. 10. EXPANDED VIEW OF TRANSVERSE AND STREAMWISE CORRELATIONS IN A SUPERSONIC FREE SHEAR LAYER. (a) DOWNSTREAM VELOCITY CORRELATION, (b) UPSTREAM VELOCITY CORRELATION WITH THE DOWNSTREAM VELOCITY, (c) UPSTREAM VELOCITY CORRELATION, (d) DOWNSTREAM CORRELATION WITH THE UPSTREAM VELOCITY.

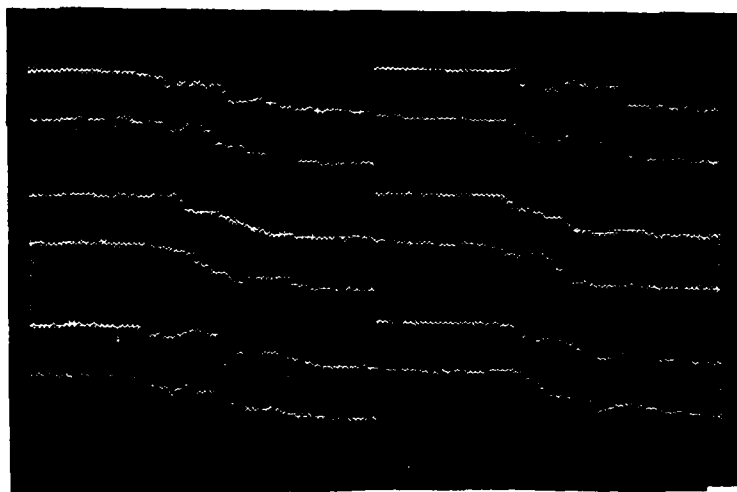


FIG. 11. TAGGED LINE PAIRS ACROSS A HIGH-SPEED SUBSONIC FREE SHEAR LAYER. OVERLAID BRIGHT PIXELS INDICATE THE COMPUTER-IDENTIFIED LINE POSITION.

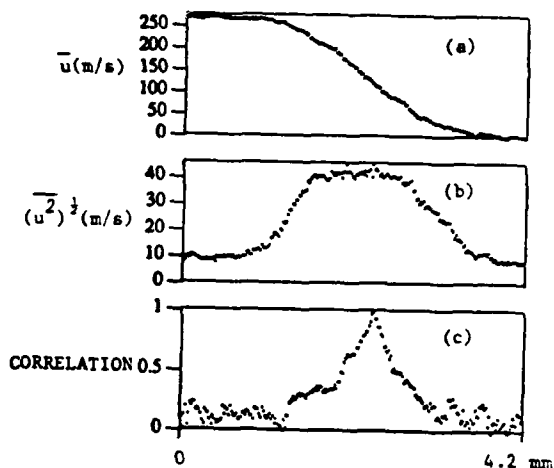


FIG. 12. (a) AVERAGE VELOCITY, (b) TURBULENCE INTENSITY, AND (c) VELOCITY CORRELATION ACROSS A SUBSONIC FREE SHEAR LAYER 11.5 mm DOWNSTREAM OF THE NOZZLE EXIT.

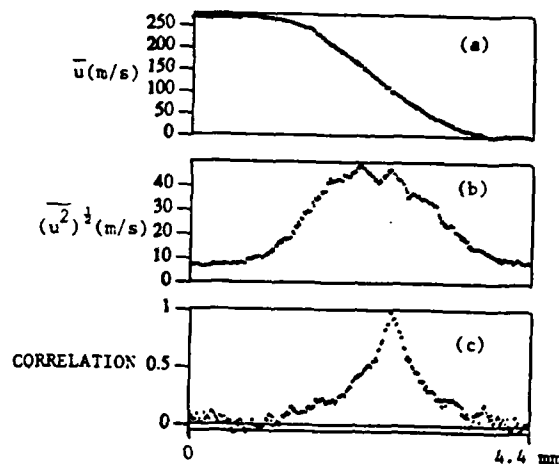


FIG. 13. (a) AVERAGE VELOCITY, (b) TURBULENCE INTENSITY, AND (c) VELOCITY CORRELATION ACROSS A SUBSONIC FREE SHEAR LAYER 12.2 mm DOWNSTREAM OF THE NOZZLE EXIT.

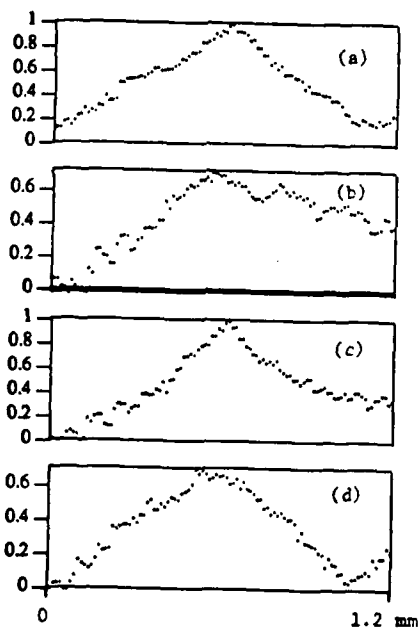


FIG. 14. EXPANDED VIEW OF TRANSVERSE AND STREAMWISE CORRELATIONS IN A SUBSONIC FREE SHEAR LAYER. (a) DOWNSTREAM VELOCITY CORRELATION, (b) UPSTREAM VELOCITY CORRELATION WITH THE DOWNSTREAM VELOCITY, (c) UPSTREAM VELOCITY CORRELATION, (d) DOWNSTREAM CORRELATION WITH THE UPSTREAM VELOCITY.

ABSTRACTS SUBMITTED TO THE 41st ANNUAL MEETING OF
THE DIVISION OF FLUID DYNAMICS OF THE AMERICAN PHYSICAL SOCIETY

Buffalo, New York
November 1988

1. "Instantaneous and Time-Averaged Turbulent Structure in the Free Shear Layer of an Underexpanded Supersonic Air Jet."* E. MARKOVITZ, J. CONNORS, G. ROTH, P. HOWARD, and R. MILES, Princeton University--Oxygen molecular flow tagging by Raman Excitation + Laser-Induced Electronic Fluorescence (RELIEF) is used to follow the motion of the air in the free shear layer of a supersonic axisymmetric jet. By recording numerous instantaneous velocity profiles, the average velocity profile, turbulence intensity, and velocity correlation across the free shear layer are found. Measurements of the development of the free shear layer as a function of the distance downstream of the nozzle are compared with a subsonic flow to examine the effects of compressibility.

*Work sponsored by AFOSR, Grant #86-9191.

2. "Instantaneous Velocity Profiles and Density Cross Sections in High-Speed Air by RELIEF."* J. CONNORS, E. MARKOVITZ, G. ROTH, P. HOWARD, and R. MILES, Princeton University--A new method of molecular flow tagging using Raman Excitation + Laser-Induced Electronic Fluorescence (RELIEF) enables us to instantaneously write lines in high-speed air flows and analyze their motion in a manner similar to what is done with hydrogen bubbles in a water flow channel. The tagging step vibrationally excites oxygen molecules which then move downstream until they are interrogated by laser-induced electronic fluorescence. The interrogation laser also gives a density cross section of the flow by Rayleigh scattering. Examples will be shown in high-speed air flows up to Mach 3.6 using both single and double line marking. By recording numerous instantaneous velocity profiles, the time-averaged velocity and turbulent statistics can be computed. Extensions of the RELIEF technique to the measurement of vorticity, temperature, and three-dimensional structure will be discussed.

*Work supported by AFOSR, Grant #86-0191.